

Research Article

Evaluation and Formulation of Assessment Criteria for Dominant Distresses in Preventive Maintenance of Cement Concrete Pavements

Qiqi Chen ¹, Guanhu Wang ¹, Xuelin Huang ¹, Guanpeng Wang ², and Ke Li ¹

¹School of Aeronautical Engineering, Air Force Engineering University, Shaanxi, Xi'an 710038, China

²Shandong Provincial Institute of Land Surveying and Mapping, 2301, Lingang South District, Jingshi Road, Jinan, China

Correspondence should be addressed to Guanhu Wang; kgdwgh@163.com

Received 29 June 2020; Revised 31 October 2020; Accepted 24 November 2020; Published 10 December 2020

Academic Editor: Ramon Sancibrian

Copyright © 2020 Qiqi Chen et al. This is an open access article distributed under the Creative Commons Attribution License, which permits unrestricted use, distribution, and reproduction in any medium, provided the original work is properly cited.

Different types of distresses affect cement concrete pavement at different degrees. The determination of dominant distresses of the pavement preventive maintenance (PM) and its judgement standard can provide corresponding basis for PM decision. In this paper, 22 military airports in Northeast China, such as Heilongjiang Province, Jilin Province, and Liaoning Province, were selected to collect the data of pavement distresses. Based on the structural equation model (SEM), the structural relationship between the influencing factors of each distress and the pavement damage was established, and the goodness-of-fit of the model was tested. In addition, through path analysis, the influence degree of five kinds of latent variables such as joint distress, surface distress, vertical distress, repair distress, and fracture distress on pavement damage was obtained. Four distresses, such as corner peeling, surface peeling, surface crack, and interplate slip, were identified as the dominant distresses of PM of cement concrete pavement. On this basis, a binary classification model of confusion matrix was constructed. The basic evaluation index, receiver operating characteristic (ROC) curve, and Kolmogorov-Smirnov (KS) curve were used to comprehensively determine the judgement standard of the dominant distresses of pavement PM from multiple evaluation angles (corner peeling rate $\leq 35\%$, surface peeling rate $\leq 30\%$, surface crack rate $\leq 8\%$, and interplate slip rate $\leq 0.5\%$). The judgement standard can be combined with the corresponding prediction model to determine the optimal timing of PM of cement concrete pavement and provide pavement maintenance managers with the support of decision-making.

1. Introduction

The cement concrete pavement of the airport will produce various distresses in the use process inevitably. The distress will be aggravated by the combined action of wheel load and environment, leading to gradual attenuation of pavement performance, the accelerated damage of the aircraft, and the increased risk of flight safety [1]. Preventive maintenance (PM) is an advanced, scientific, and efficient conservation concept. It refers to the reasonable and planned implementation of corresponding conservation measures for existing pavement systems under the premise of a good pavement conditions, so as to achieve the purpose of delaying the attenuation of pavement performance and maintaining or improving

the pavement function. It has achieved a good applicational effect in the field of highway asphalt pavement. However, at present, the maintenance and management technology of military airport pavement is still relatively backward. PM has not been promoted and applied in the management of military airport pavement effectively. One of the important reasons is the lack of scientific and reasonable judgement standard that can guide the implementation of PM quantitatively. Therefore, it is necessary to thoroughly reveal the relationship of cement concrete pavement distress, analyze the influencing factors of pavement damage, and establish a scientific and quantifiable PM judgement standard according to the characteristics and maintenance requirements of cement concrete pavement of military airport.

At present, domestic and foreign scholars have performed a lot of research on the judgement standard of preventive maintenance [2–8]. Based on the types and characteristics of early distresses of asphalt pavement, Li et al. proposed the evaluation index system of preventive maintenance of asphalt pavement with the expert scoring method [9]. Wang et al., aiming at the lack of specific evaluation standard for preventive maintenance, studied the relationship among distresses, and defined the range of performance indexes for preventive maintenance of asphalt pavement [10]. According to the evaluation standard of preventive maintenance of expressway asphalt pavement, Zhang explored and defined the critical value range of key indicators of pavement performance [11]. Fan et al. proposed a comprehensive evaluation model, which combined the evaluation indexes of pavement and the material performance in the domestic technical specifications for preventive maintenance of asphalt pavement [12]. Yu et al. proposed and demonstrated a method to evaluate the microsurface treatment of asphalt pavement based on the grey system model and grey relational degree theory and obtained the critical value of the microsurface treatment of pavement distresses [13]. Loprencipe and Zoccali used BBI, IRI, and ProFAA simulation models to evaluate the roughness of the real runway profile and explained the different effects of the results they provided on the airport pavement management. The type and scope of interventions that can restore runway flatness were correctly defined [14]. Vu-Bac et al. provided a sensitivity analysis toolbox composed of a set of Matlab functions, which is used to quantify the influence of uncertain input parameters on the output of an uncertain model. It is of great significance to defining the weights of the assessment criteria [15].

According to the analysis of the PM standards in China and abroad, at present, the PM standards mainly focus on the highway asphalt pavement. There are few studies on airport pavements, even less on cement concrete pavements, and rare on cement concrete pavements in military airports. The majority of researchers adopt qualitative or semiquantitative methods to determine the PM standards, while few studies adopt quantitative methods to accurately calculate the PM standards. The objectives of the current study are as follows: (1) determine the influencing factors affecting the pavement damage of the military airport in the seasonal frozen area and categorize the factors into groups; (2) establish a structural equation model (SEM) to describe the relationship between pavement damage and the influencing factors; (3) evaluate the effect of each influencing factor and determine the dominant distresses of pavement PM; (4) establish the confusion matrix model to classify the judgement results; and (5) according to the ROC curve and other evaluation indexes, determine the judgement standard of the dominant distresses of pavement PM comprehensively.

As a statistical data analyzing tool, not only can SEM analyze the complex structural relations among latent variables but it also estimates the factor structure and factor relations. In addition, the measurement error can be

analyzed and processed to estimate the fitting degree of the whole model [16, 17]. Lu and Kang established a structural equation model to explore the interrelationship of organizational factors in management projects and obtained the positive influence of the project diversity and the interdependence of project complexity [18]. The confusion matrix model is a common model to evaluate the performance of the classifiers. It contains rich information about intraclass aggregation and interclass dispersion. It can describe the relationship between the real attributes of sample data and the types of recognition results [19, 20]. Sisodia and Sisodia built a confusion matrix model to solve problems such as the complicated process of diabetes recognition and predicted the probability of people developing diabetes by evaluating indexes such as accuracy and recall rate [21].

In conclusion, SEM and the confusion matrix model have good applications in exploring the complex structural relations among variables and predicting the threshold of variables. Therefore, on the basis of referring to the existing achievements, this paper establishes SEM to clarify the relationship among cement concrete pavement distresses and quantitatively determine the dominant distresses of PM of military airport pavement. On this basis, the confusion matrix model is constructed. The basic evaluation index, ROC curve, and KS curve are used to determine the judgement standard of the dominant distress of pavement PM, so as to provide the corresponding basis for quantitative guidance of PM implementation and provide pavement maintenance managers with the support of decision-making.

This paper attempts to develop two new mathematical models (structure equation model and confusion matrix model) and apply them to the relationship among pavement distresses, which has not been performed by previous researchers. The research area of this paper is 22 military airports in the seasonal frozen area. By now, no one has studied the relationship among the distresses of the military airports in the seasonal frozen area and has determined the dominant distress of PM of cement concrete pavement and its judgement standard. Through the analysis of the solution results of the structural equation model and confusion matrix model, it is found that the fitting degree conforms to the recommended value, which verifies the research hypothesis proposed in this paper. The research results of this paper have the military application value. This paper quantitatively analyzes the relationship between the distress and the pavement, identifies the dominant distress of PM of cement concrete pavement and its judgement standard, and determines the key content of the maintenance of military airport pavement. It can greatly improve the service life of the pavement and lay a foundation for ensuring the safe take-off and landing of the military aircraft.

The rest of the paper is organized as follows. Section 2 introduces the data sources, methodological overview, and approach based on SEM and the confusion matrix model. Section 3 introduces the principle of the SEM, analyzes the relationship among the cement concrete pavement distresses by constructing SEM, and quantitatively determines the dominant distresses of PM of the pavement. In Section 4, the

confusion matrix model is constructed, and the judgement standard of the dominant distress of pavement PM is determined by the basic evaluation index, ROC, and KS curve. Conclusions are presented in the final section.

2. Materials and Methods

2.1. Study Area. With the vast territory of China, the natural conditions in different regions are different. Therefore, it is necessary to study the dominant distress and its judgement standard of the PM of the cement concrete pavement of the military airport according to different regional conditions. The seasonal frozen area in China has a wide distribution and many types, accounting for more than 50% of the total land area in China. A large number of military airports are located in the seasonal frozen area. Due to the complexity of natural conditions in the seasonal frozen area, the variety of damage forms and the complexity of deterioration factors of the surface performance are caused. To study the relationship of cement concrete pavement distress of military airfields in the seasonal frozen region and then determine the dominant pavement distress and its judgement standard of PM, this paper investigated military airfields in the seasonal frozen region of Northeast China, such as Heilongjiang Province, Jilin Province, and Liaoning Province. 22 airports (No. 1–22, the distribution is shown in Figure 1 [22]) were selected as sample airports, and relevant pavement distress data were collected.

As can be seen from Figure 1, all sample airports are within the scope of the northeast seasonal frozen area. Most of the sample airports are concentrated in the southeast of the northeast seasonal frozen area, among which there are a large number of sample airports in Liaoning and Jilin Provinces with a relatively dense distribution. There are four sample airports in Heilongjiang Province and one in eastern Inner Mongolia. Among them, No. 19 and No. 22 are alternate airports, and the rest are common airports. No. 4, 5, 10, 16, 17, 18, and 21 are civil and military airports. It can be seen that the type and distribution range of the 22 sample airports selected in this paper are reasonable and fully representative.

2.2. Methods. The survey data were sourced from 22 sample airports in the northeast seasonal frozen area, including the types and causes of pavement distresses in military airports over the years. Questionnaire survey and face-to-face interview were conducted for airport staff. The questionnaire contained two parts: basic personal information and cement concrete pavement damage information. The first part is the basic personal information, including gender, age, educational background, occupation, and position. In order to ensure the professionalism and effectiveness of the collected questionnaire data, 60% of the total respondents are technical personnels engaged in pavement maintenance, and they have more than 5 years of work experience. The administrative leadership of the pavement maintenance department accounts for 20%, and they are familiar with the pavement conditions of the

airport. Pilots account for 20%. They are users of the pavement, and they know more about the wear of the plane on the pavement. Obtaining data from them is more in line with the actual situation of the airport pavement. The second part is information of influencing factors of cement concrete pavement damage (main distress types of pavement damage and corresponding specific distresses). The questionnaire also included some open-ended questions, such as whether there was currently a judgement standard in PM of pavement, and if so, what was the basis.

The research method and process of this paper are shown in Figure 2, which can be divided into two stages:

- (i) Stage 1 (analyze the relationship of pavement distresses and determine the dominant distress of PM). First, data collection was carried out to get the data needed in this study. Second, the SEM and its basic principle were introduced. Through the questionnaire survey, variable analysis, and research hypothesis, the model was constructed and solved. Furthermore, the model fitting index test and path analysis were carried out to determine the dominant distress in PM of cement concrete pavement.
- (ii) Stage 2 (determine the dominant distress judgement standard). The basic principle of the confusion matrix was introduced, and the model was constructed. In addition, the basic evaluation index, the ROC curve, and the KS curve were used to comprehensively determine the judgement standard of the dominant distress of pavement PM from multiple evaluation angles.

3. Analysis of Dominant Distresses in Preventive Maintenance of Cement Concrete Pavement

3.1. Structural Equation Model. Many kinds of distresses affect the damage of cement concrete pavement, but none of them can be directly measured. Moreover, the mechanism of each distress factor to cement concrete pavement is complex, which is difficult to deal with by the traditional multiple regression analysis technology. The SEM can establish the relationship between measurement variables and latent variables. Although the latent variable cannot be measured directly because of its abstract features, it can be analyzed by measuring the observed variables. Observed variables can be measured by a questionnaire. In multivariate statistical analysis, the causal relationship among variables can be better tested by modeling measurement errors [23, 24]. Therefore, SEM was chosen as the analytical method in this paper.

A complete SEM model includes a measurement model and a structural model. The measurement model describes the interrelationship between observed variables and latent variables, while the structural model describes the relationship among different latent variables [25, 26]. Here, equations (1) and (2) represent the measurement model, and equation (3) represents the structural model:

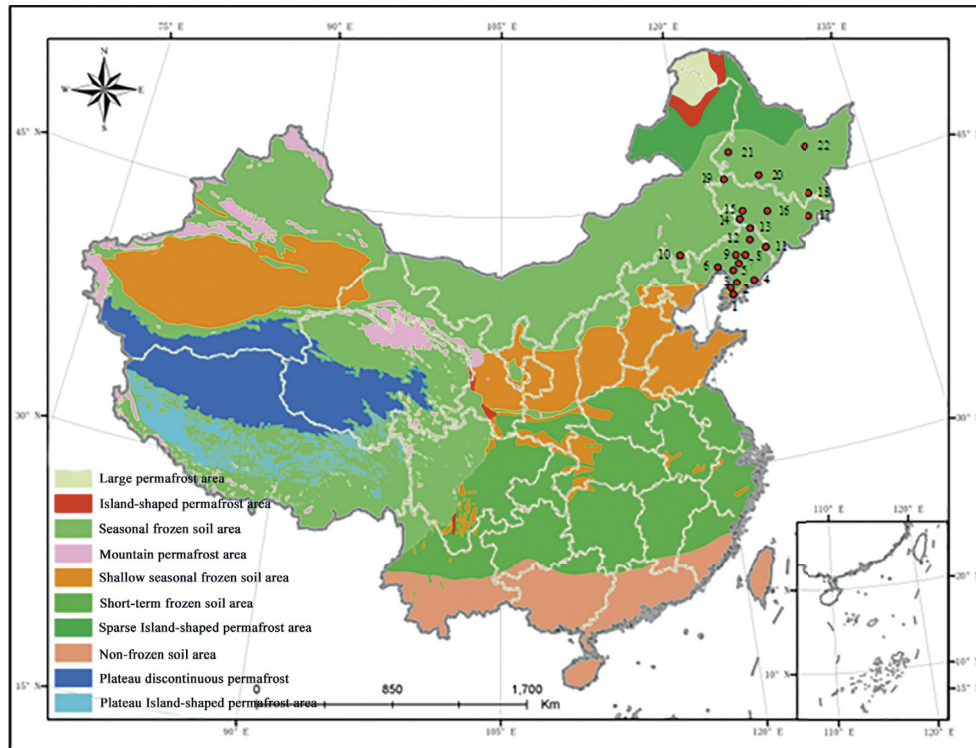


FIGURE 1: Schematic diagram of sample airport distribution.

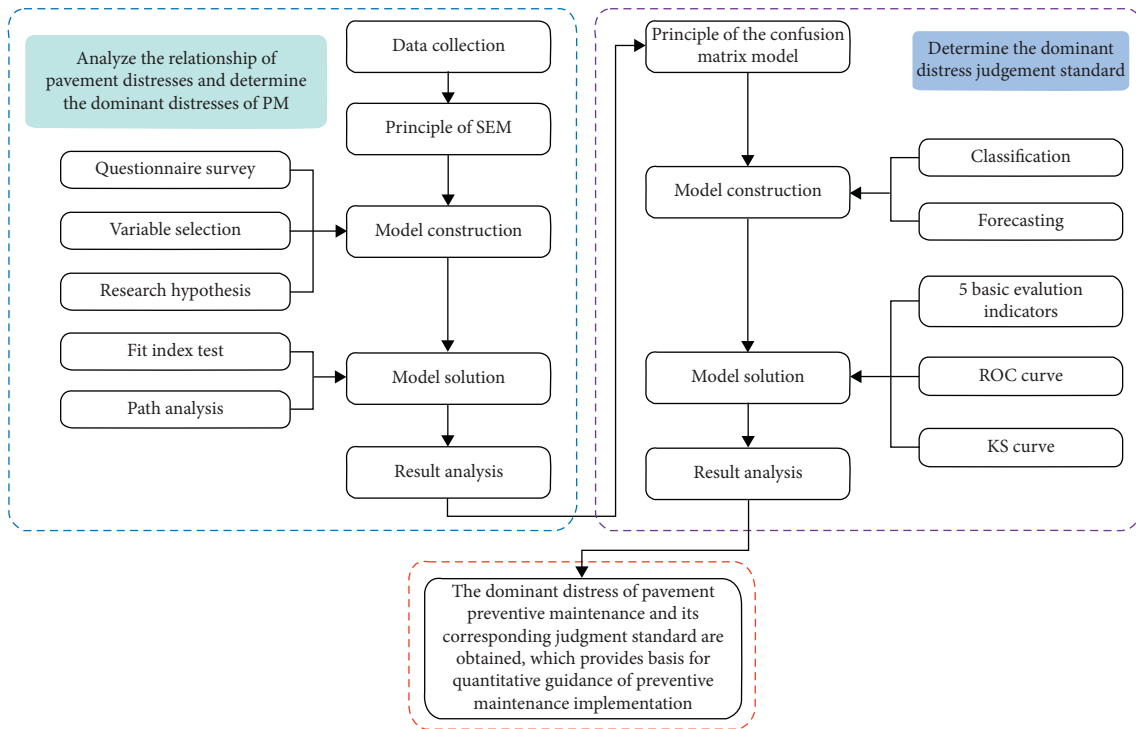


FIGURE 2: Schematic framework of methodology approach for pavement dominant distress and its judgement standard.

$$x = \Lambda_x \xi + \delta, \quad (1)$$

$$y = \Lambda_y \eta + \varepsilon, \quad (2)$$

$$\eta = B\eta + \Gamma\xi + \zeta, \quad (3)$$

where Λ_x is the factor load matrix of the exogenous variable x , ξ is used as a latent exogenous variable, δ is the error vector of the exogenous variable, Λ_y is the factor load matrix of the endogenous variable y , η is an latent endogenous variable, ε is the error vector of the endogenous variable, B is the coefficient matrix of latent endogenous variables, Γ is the coefficient matrix of latent exogenous variables, and ζ is the error vector.

3.2. Model Construction and Solution

3.2.1. Model Construction. In this study, questionnaires were distributed to 22 sample airports, and 865 questionnaires were recovered. Excluding 23 questionnaires with more abnormal values, a total of 842 valid questionnaires were obtained. After analysis by SPSS software, Cronbach's coefficient of the total questionnaire reached 0.91, which was above the specified value of 0.8 [27]. It indicates that the questionnaire of this study has a good overall reliability.

According to the existing theoretical research results and the data of cement concrete pavement damage in military airport in the seasonal frozen area obtained through practical investigation, the following main factors influencing pavement damage were summarized:

- (1) Joint distresses. Cement concrete pavement often has a large number of joints during construction. The joint filler of the newly built airport will gradually age under the long-term erosion of the natural environment (especially the freeze-thaw cycle and frost heaving in the seasonal frozen zone). It is easy to produce problems such as corner peeling, joint filler damage, and mud around the joint, so that the joint is a part of the cement concrete pavement which is prone to damage [2].
- (2) Surface distresses. Due to the large temperature difference between day and night in the seasonal frozen area, the temperature changes cause thermal expansion and contraction of the cement concrete pavement panels, resulting in subtle cold shrinkage cracks. Under the repeated effects of aircraft loads and rain, small cracks will deteriorate into big cracks. Moreover, under the repeated action of the freeze-thaw cycle, local stress concentration on the pavement causes slight erosion of the surface layer until significant peeling damage occurs [4].
- (3) Vertical distresses. In the seasonal frozen area, due to the influence of the complex climate, the moisture in the soil foundation under the pavement in autumn and winter will migrate under the action of the temperature gradient. The water condenses into ice during freezing, and the volume increases continuously, which leads to the expansion of the soil

foundation. When the frost heaving amount of soil foundation reaches a certain degree, the slip phenomenon among pavement panels occurs. In spring and summer, as the temperature field changes, the ice crystals accumulated in the soil base gradually melt. The pore in soil base increases and the bearing capacity decreases. Under the repeated action of the aircraft wheel load, the soil foundation sinks and gradually forms a bottom void. As the season alternates repeatedly, the effects of frost heaving and sinking are repeated, which will cause the bottom of the pavement panel to be emptied and staggered [6].

- (4) Repair distresses. Repair distresses refer to small patches and large patches. The small patch refers to the repair of the partially damaged surface. The large patch refers to a pavement surface that is repaired after excavation of the original pavement due to the addition of underground pipelines and other facilities [2].
- (5) Fracture distresses. The airport with serious pavement damage often has more plate fracture distresses. When surface distresses such as surface cracks and surface spalling occur and they are not repaired in time, with the comprehensive action of water intrusion and load fatigue, surface distresses continue to exacerbate, cracks continue to expand and become deeper, and the bearing capacity of soil foundation under the pavement panel continues to decline. And all of these lead to distresses such as plate bottom emptying and slippage. With the continuous comprehensive action of water intrusion and load, the structural damage of the pavement, such as plate angle fracture, plate fracture, and even plate fragmentation, will eventually occur [7].

Therefore, based on the multilevel features of pavement damage, this paper divided the factors affecting pavement damage into five latent variables: joint distress, surface distress, vertical distress, repair distress, and fracture distress. The interaction of these five factors will accelerate the pavement damage and reduce the service life of the pavement. In this paper, the damage evaluation indicators of cement concrete pavement of military airport in the seasonal frozen area were constructed. Joint distress, surface distress, vertical distress, repair distress, fracture distress, and pavement damage were selected as the core latent variables of the pavement damage model. And eight research hypotheses were proposed for the conceptual model:

- (i) Hypothesis 1 (H1): joint distresses have a positive impact on pavement damage
- (ii) Hypothesis 2 (H2): surface distresses have a positive impact on pavement damage
- (iii) Hypothesis 3 (H3): vertical distresses have a positive impact on pavement damage
- (iv) Hypothesis 4 (H4): repair distresses have a positive impact on pavement damage
- (v) Hypothesis 5 (H5): fracture distresses have a positive impact on pavement damage

TABLE 1: Characteristic description and typical legends of pavement distress.

Latent variables	Observed variables	Feature description	Typical legend
	Corner peeling (Joi1)	It refers to the damage caused by cutting the plate thickness at an oblique angle instead of through the plate thickness at the edge and corner of the plate	
Joint distress (Joi)	Mud (Joi2)	Base material is deposited near the joints or cracks	
	Joint filler damage (Joi3)	Under the combined effect of environmental and load factors, the joint filler loses its elasticity and plugging effect	
Surface distress (Sur)	Surface peeling (Sur1)	Spalling, exposed stones, and potholes on the surface of the plate, which damage the flatness of the pavement surface	
	Surface crack (Sur2)	There are shallow cracks on the plate surface that do not penetrate the thickness of the plate. This kind of crack does not affect the bearing strength of the plate	
Vertical distress (Ver)	Interplate slip (Ver1)	Uneven vertical displacements at the joints of adjacent plates	
	Void at the bottom of panel (Ver2)	Significant plate movements as aircraft wheels pass near cracks	
Repair distress (Rep)	Secondary distress of the patch (Rep1)	Local repairs on the plate	
Fracture distress (Fra)	Plate fragmentation (Fra1)	It refers to the cracks that run through the thickness of the plate in the noncorner of the plate, forming more than 4 pieces of broken pieces, which have completely lost the original bearing capacity	
	Plate fracture (Fra2)	There are cracks in the vertical and horizontal direction that penetrate through the thickness of the plate. Usually, there are 1 or 2 cracks, which cause the plate to crack into 2 or 3 pieces	
	Plate angle fracture (Fra3)	There are cracks through the thickness of the plate at the corner of the plate. The corner of the plate is broken. The side length of the corner is 1/10-1/2 of the plate length, about 50-100 cm	
Pavement damage (Pav)	—	—	—

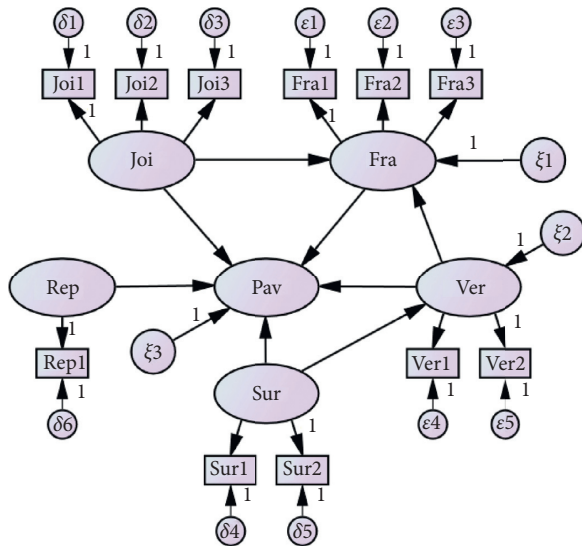


FIGURE 3: Path diagram of factors affecting pavement damage.

- (vi) Hypothesis 6 (H6): surface distresses have a positive impact on vertical distresses
- (vii) Hypothesis 7 (H7): vertical distresses have a positive impact on fracture distresses
- (viii) Hypothesis 8 (H8): joint distresses have a positive impact on fracture distresses

Based on the above hypothesis, the distress types and its full path diagrams affecting the damage of cement concrete pavement were obtained, as shown in Table 1 and Figure 3, respectively. It can be seen from Table 1 that the SEM has a total of 6 potential variables and 11 observed variables.

3.2.2. Model Solution. Based on the data obtained from the survey, the database of 842 sample data was established in SPSS software. At the same time, it was imported into AMOS software to solve the model. This paper mainly applied the path analysis method, analyzed the dominant distress factors affecting pavement damage, and studied the relationship among various distress factors and their influencing effects through path diagram and effect value. The effect values are divided into direct effect, indirect effect, and total effect. Each effect represents different effects among variables. The calculated model fitting index is shown in Table 2. The six indexes in the table, respectively, reflect the model precision from different aspects. Through the analysis of the six types of commonly used model fitting evaluation index, the model fitting accuracy in this paper was evaluated.

Generally, absolute fit, incremental fit, and parsimonious fit are used to judge the fitness of a model. The model was measured by different fit indexes. As can be seen from Table 2, the chi-square/df ratio (χ^2/df) of 2.349 and the goodness-of-fit (GFI) index value of 0.952 indicate an acceptable fit of the data. Furthermore, the values of all other essential indices, including root mean square error of approximation (RMSEA), comparative fit index (CFI), normed fit index (NFI), and parsimony goodness-of-fit index (PGFI)

are above their respective threshold values, which strongly support the satisfactory fit between the measurement model and the data [17].

Figure 3 shows the influence path of various factors on the damage of cement concrete pavement. The direct effect, indirect effect, total effect, and load matrix of each factor on pavement damage are shown in Tables 3 and 4, respectively.

3.3. Results and Discussion. The influence path and strength of each factor on pavement damage are analyzed as follows. The path coefficients of joint distress, surface distress, vertical distress, repair distress, and fracture distress are 0.244, 0.337, 0.261, 0.093, and 0.065, respectively, which means that for every standard deviation (S.D.) of joint distress, surface distress, vertical distress, repair distress, or fracture distress, the pavement damage will increase by 0.244, 0.337, 0.261, 0.093, or 0.065 S.D. The positive coefficient indicates that the degree of pavement damage increases with the increase of joint distresses, surface distresses, vertical distresses, repair distresses, or fracture distresses, which supports our research hypothesis 1–5. The direct effects of surface distresses on vertical distresses and joint distresses and vertical distresses on fracture distresses are 0.100, 0.120, and 0.150, respectively. This supports hypothesis 6–8. In addition, joint distresses, surface distresses, and vertical distresses have a significant positive impact on pavement damage, while repair distresses and fracture distresses have a weak positive impact. The direct effects of joint distresses and vertical distresses on pavement damage are 0.236 and 0.251, respectively. The indirect effects of joint distresses and vertical distresses on pavement damage through fracture distresses are 0.008 and 0.010, respectively. The total effects are 0.244 and 0.261, respectively. The higher path coefficient indicates that the joint distresses and the vertical distresses are the main factors affecting the pavement damage. In the joint distresses, the factor load value of corner peeling is larger, which is 0.846. In the vertical distresses, the factor load value of interplate slip is larger, which is 0.730. They are a better representative of joint distresses and vertical distresses, respectively. The direct effect of surface distresses on pavement damage is 0.311, the indirect effect through vertical distresses is 0.026, and the total effect is 0.337. Its path coefficient is the largest, which indicates that it is the most important factor affecting the pavement damage. In the surface distresses, the factor loads of surface peeling and surface cracks are large, which can better represent the surface distresses.

The effects of fracture distresses and repair distresses on pavement damage are low. This is because the distresses targeted at the PM of cement concrete pavement are not necessarily the typical or the most serious distresses, but the dominant distresses, which are the potential hidden trouble that makes the pavement structure function decay. Therefore, early distresses of joint distresses and surface distresses should be paid attention to first, followed by medium distresses of repair distresses and vertical distresses, and late distresses of fracture distresses should not be considered generally. Repair distresses are essential secondary distresses, which are not strictly within the scope of PM, so they are not considered.

TABLE 2: Model fit indices of the proposed model.

Measures	Fit index	Description	Model index	Recommend level [28]	Model adaptation judgement
Absolute fit measures	χ^2/df	Check whether the covariance structure of the model is adequately the same as the covariance matrix of the observed data	2.349	<5	Support
	GFI	Check the overall fit of the model	0.952	>0.90	Support
	RMSEA	Check the mean value of the covariance residual	0.061	<0.08	Support
Incremental fit measures	CFI	Examine whether the model fits the observed data better than the independent model that has no relationships among variables	0.943	>0.90	Support
	NFI	Explore the improvement of the overall fit of the model to the independent model	0.916	>0.80	Support
Parsimonious fit measures	PGFI	Examine the overall parsimony of the model	0.72	>0.50	Support

TABLE 3: Standardized direct, indirect, and total effects.

	Surface distress	Vertical distress	Joint distress	Fracture distress	Repair distress
Surface distress					
Direct effect	NA	NA	NA	NA	NA
Indirect effect	NA	NA	NA	NA	NA
Total effect	NA	NA	NA	NA	NA
Vertical distress					
Direct effect	0.100	NA	NA	NA	NA
Indirect effect	0.000	NA	NA	NA	NA
Total effect	0.100	NA	NA	NA	NA
Joint distress					
Direct effect	NA	NA	NA	NA	NA
Indirect effect	NA	NA	NA	NA	NA
Total effect	NA	NA	NA	NA	NA
Fracture distress					
Direct effect	0.000	0.150	0.120	NA	NA
Indirect effect	0.015	0.000	0.000	NA	NA
Total effect	0.015	0.150	0.120	NA	NA
Repair distress					
Direct effect	NA	NA	NA	NA	NA
Indirect effect	NA	NA	NA	NA	NA
Total effect	NA	NA	NA	NA	NA
Pavement damage					
Direct effect	0.311	0.251	0.236	0.065	0.093
Indirect effect	0.026	0.010	0.008	0.000	0.000
Total effect	0.337	0.261	0.244	0.065	0.093

Note. "NA" denotes "not applicable."

Based on the above analysis, this paper finally determined that four distresses, including corner peeling, surface peeling, surface crack, and interplate slip, are the dominant distresses in PM of cement concrete pavement of military airfields in the seasonal frozen area.

4. Determination of Dominant Distresses Judgement Standard

4.1. Confusion Matrix. Confusion matrix is a situation analysis table that summarizes the result of the classification model in machine learning and records the data in the form of matrix. The row of the matrix represents the judgement value, and the

column of the matrix represents the actual value [29, 30]. The basic model is shown in Table 5.

False-positive rate (FPR) = FP/FP + TN, the proportion of actual negatives that are misclassified.

For the confusion matrix model, the basic evaluation index, the ROC curve, and the KS curve are generally used to evaluate it from the aspects of classification ability and model judgement accuracy.

4.1.1. Basic Evaluation Index. The basic evaluation indexes and meanings of the confusion matrix are shown in Table 6 [31].

TABLE 4: Factor load values.

Latent variables	Observed variables	Factor load values
Joint distress	Corner peeling	0.846
	Mud	0.379
	Joint filler damage	0.391
Surface distress	Surface peeling	0.738
	Surface crack	0.752
Vertical distress	Interplate slip	0.730
	Void at the bottom of panel	0.450
Repair distress	Secondary distress of the patch	0.624
Fracture distress	Plate fragmentation	0.691
	Plate fracture	0.722
	Plate angle fracture	0.754

TABLE 5: Confusion matrix.

Confusion matrix	Actual value	Positive	Negative	Total
Judgement value	Positive	True-positive (TP)	False-positive (FP)	TP + FP
	Negative	False-negative (FN)	True-negative (TN)	FN + TN
	Total	TP + FN	FP + TN	TP + FP + FN + TN

TABLE 6: Description of evaluation metrics.

Index	Calculation formula	Description
Accuracy (ACC)	Accuracy = ((TP + TN)/(TP + FP + TN + FN))	It refers to the ratio of the number of correctly classified cases
Precision (positive predictive value, PPV)	Precision = (TP/(TP + FP))	It refers to the proportion of judging positives that are correctly identified
Recall (true-positive rate, TPR)	Recall = (TP/(TP + FN))	It refers to the proportion of actual positives that are correctly identified
Specificity (true-negative rate, TNR)	Specificity = (TN/(TN + FP))	It refers to the proportion of actual negatives that are correctly identified
F1 score	F1 = (2 * precision * recall)/(precision + recall)	It is a tradeoff between precision and recall

4.1.2. *ROC Curve and KS Curve.* The ROC graphic depicts the tradeoff between TPR and FPR and drawn on x and y axes in the l leaner scale. In other words, one classifier cannot increase the number of true-positives without increasing the false-positives. In a ROC curve, the x -axis represents the FPR and the y -axis represents the TPR. Each point on the ROC curve corresponds to a result of the model. The best performance model is when the ROC curve passes through or close to (0, 1). The point (0, 1) indicates that the model judgement value is completely consistent with the actual value. The combination of a completely random prediction point will result in a 45° obliquity line, and the corresponding accuracy of any point on this line is 50%. In the KS curve, the x -axis represents the sample threshold and the y -axis represents the TPR and FPR. According to different sample thresholds, the corresponding TPR and FPR are calculated to obtain the KS curve. The maximum value of the difference between TPR and FPR curve is the KS value, and the corresponding threshold is the optimal threshold. Generally, if the KS value is greater than 0.2, the model is considered to have good accuracy. The ROC and the KS curves are shown in Figure 4.

4.2. *Construction and Solution of the Confusion Matrix Model*

4.2.1. *Model Construction.* Combined with the problems studied in this paper, the definition of “positive” means that the PM is needed, while “negative” means that the PM is not needed. Since there was no comprehensive judgement standard for pavement PM in the current specifications, the pavement damage index, as a comprehensive dimension index, can reflect the damage condition of pavement on the whole. Therefore, this paper selected the judgement standard in PM of pavement damage index. The qualified data judged by the standard are the samples that need PM in the actual value, while the unqualified data are the samples that do not need PM in the actual value.

Based on the collected dominant distress data, each time a sample threshold is given, data below the threshold determine that the PM is required, and data above the threshold determine that the PM is not required [32]. Taking the corner peeling rate (P_{cp}) as an example, TP represents the number of samples that both the judgement value and the actual value need PM when a threshold value of P_{cp} is given; FP represents the number of samples that the judgement

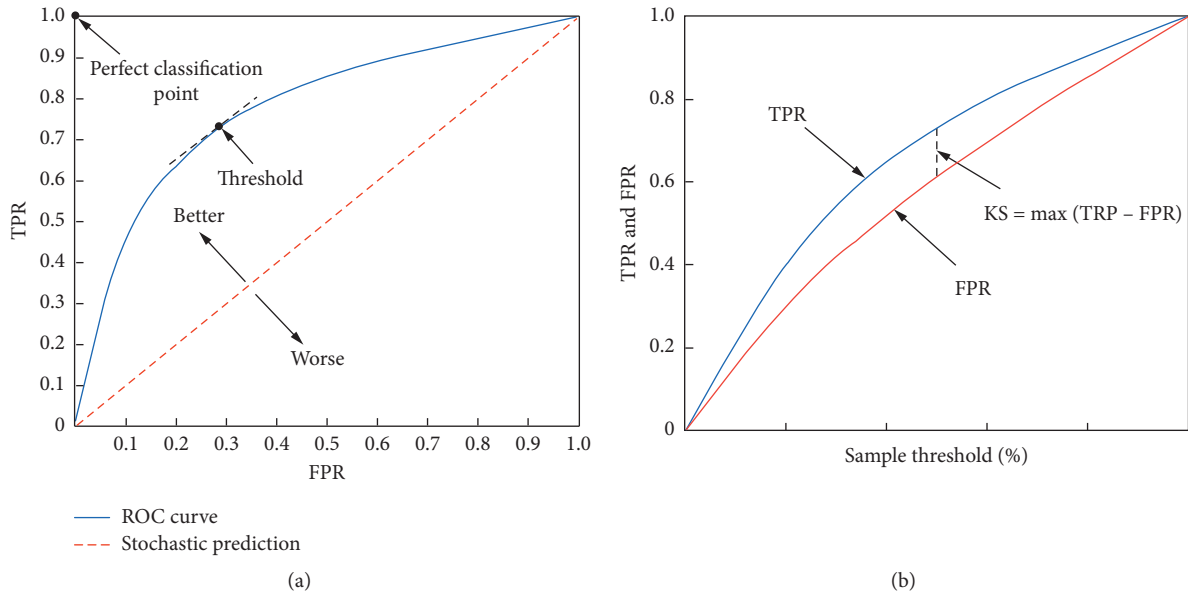


FIGURE 4: The ROC and the KS schematic diagram. (a) ROC schematic diagram (b) KS schematic diagram.

value needs PM but the actual value does not; FN represents the number of samples that the actual value needs PM but the judgement value does not; and TN represents the number of samples that both the judgement value and actual value do not need PM. The curves of ACC, PPV, TPR, TNR, $F1$ score, ROC, and KS were calculated by selecting different threshold values of P_{cp} [33]. Through analysis of multiple indicators, the optimal judgement threshold of P_{cp} was determined. The method for determining the optimal judgement threshold of surface peeling rate (P_{sp}), surface crack rate (P_{sc}), and interplate slip rate (P_{is}) is the same as above. When the optimal judgement threshold of the dominant distress is obtained, the PM judgement standard of the dominant distress can be obtained.

4.2.2. Results and Discussion. (1) The optimal judgement threshold of P_{cp} : using the measured data to calculate through the confusion matrix model, the change of the basic evaluation index of P_{cp} was obtained, as shown in Figure 5.

As can be seen from Figure 5, the ACC and the PPV increase first and then decrease with the increase of the threshold. When the threshold is 25%, the ACC reaches 0.67. That is, the sample whose judgement value is consistent with the actual value accounts for 0.67 of the total sample. The PPV reaches 0.60. Among the results whose judgement value is “PM is needed,” the proportion of correct judgement is 0.60. At the threshold of 35%, the ACC reaches the maximum value of 0.77 and the PPV reaches the maximum value of 0.65, indicating that the probability of correct judgement is relatively large.

The TPR increases first and then remains unchanged with the increase of the threshold. When the threshold is

25%, the TPR reaches 0.69. That is, among the results whose actual value is “PM is needed,” the proportion of correct judgement is 0.69. When the threshold value is 35%, the TPR reaches the maximum value of 1. As the threshold continues to increase, the TPR keeps 1 unchanged. Therefore, the optimal threshold is 35%–100%. The $F1$ score is a comprehensive judgement index of PPV and TPR, and its change trend first increases and then decreases with the increase of threshold. When the threshold is 35%, there is a maximum proportion of 0.78.

By analyzing the changes of ACC, PPV, TPR, and other indexes, it can be seen that when the threshold value of P_{cp} is 35%, the prediction accuracy of the model is higher. As an auxiliary indicator, TNR reaches 0.59 when the threshold is 35%. That is, among the results whose actual value is “no need for PM,” the proportion of correct judgement is 0.59. In the whole process of curve change, it is within the acceptable range, which verifies that 35% is the best decision threshold. Therefore, after analyzing the basic evaluation indexes, the optimal decision threshold is initially determined to be 35%, and the final decision threshold should be combined with the ROC curve and the KS curve.

The ROC curve and the KS curve of P_{cp} are shown in Figure 6.

As can be seen from Figure 6(a), the ACC corresponding to any point on the upper right 45° inclination line is 50%. Move along the 45° inclination until the point where the FPR is the smallest and the TPR is the largest. That is, the point closest to the upper left corner, with coordinates of (0.41, 1). At this time, the model has the highest prediction accuracy, and the optimal threshold corresponding to the point is 35%.

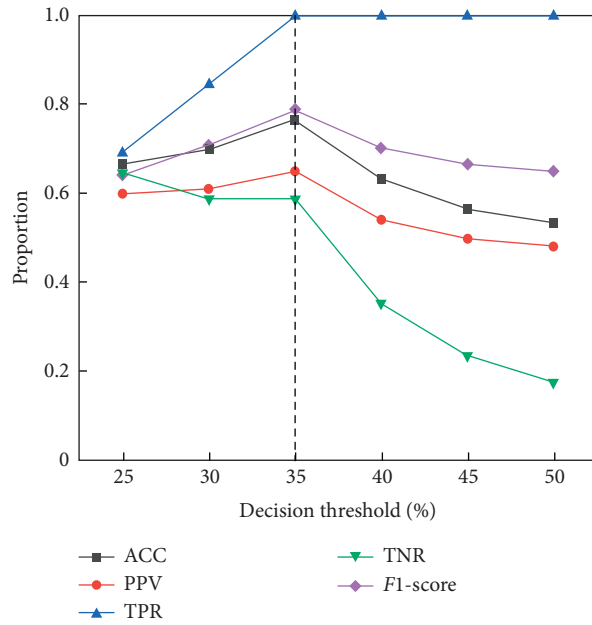


FIGURE 5: Basic evaluation index curve of P_{cp} .

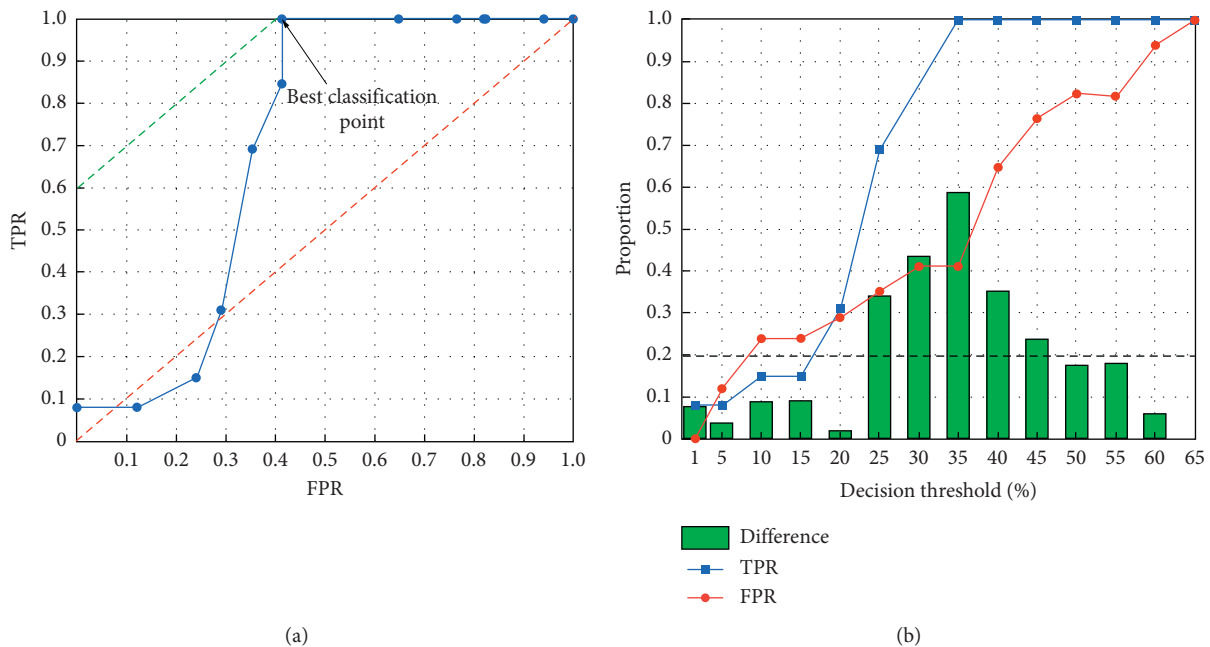


FIGURE 6: The ROC and the KS curves of P_{cp} . (a) ROC curve. (b) KS curve.

As can be seen from Figure 6(b), when P_{cp} is in the range of (25%, 45%), the difference between FPR and TPR is greater than 0.2, indicating a higher accuracy of the model. When $P_{cp} = 35\%$, the difference between FPR and the TPR reaches a maximum value of 0.59. At this time, the model is the most accurate, and the optimal threshold for P_{cp} is 35%.

Based on the above analysis of ACC, PPV, TPR, TNR, F1 score, ROC curve, and KS curve, this paper considers that 35% is the most suitable threshold for P_{cp} . The scatter diagram of $L-P_{cp}$ is shown in Figure 7. As can be seen from the

figure, when $P_{cp} \leq 35\%$, most sample points fall within the range of $3\% \leq L \leq 10\%$. It indicates that at this threshold, the success rate of correctly determining “need for PM” is higher. When $P_{cp} > 35\%$, most of the sample points fall within $L > 10\%$. It indicates that at this threshold, the success rate of correctly determining “no need for PM” is also higher. It is proved that it is reasonable to use 35% as the best threshold value of P_{cp} .

(2) The optimal judgement threshold of P_{sp} , P_{sc} and P_{is} : the solution of P_{sp} , P_{sc} , and P_{is} is the same as that of P_{cp} . The

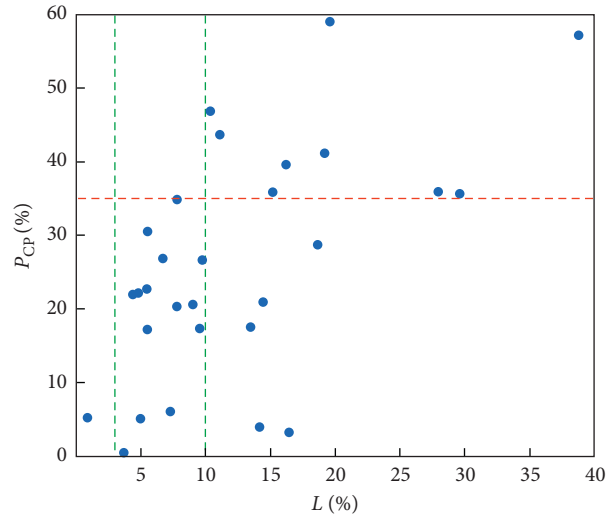
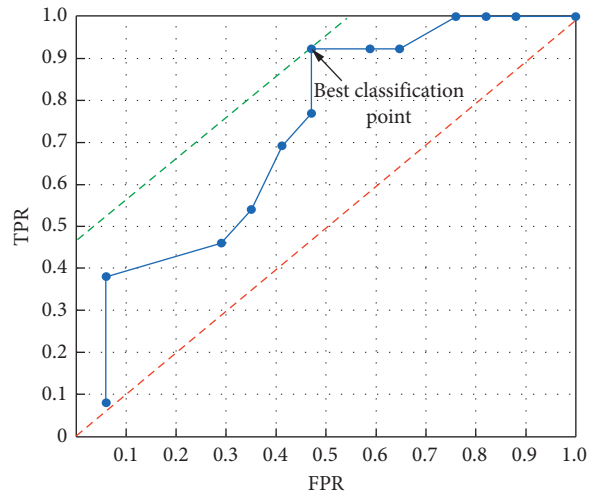
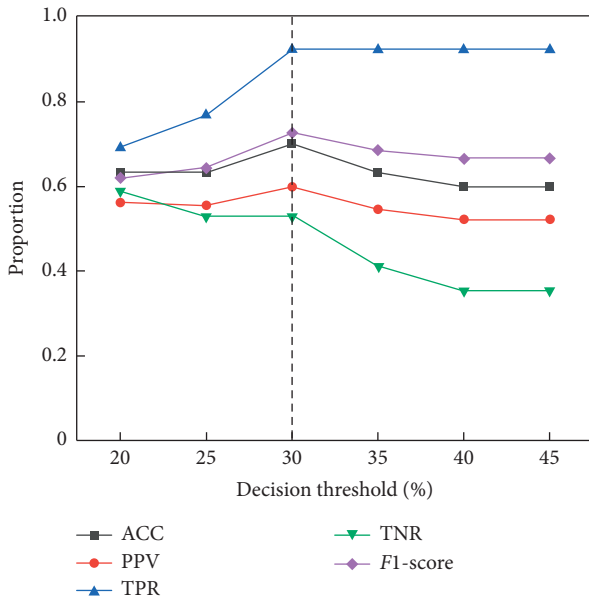


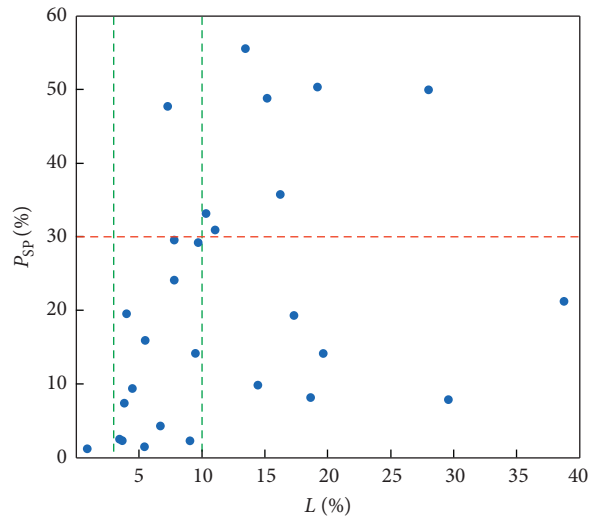
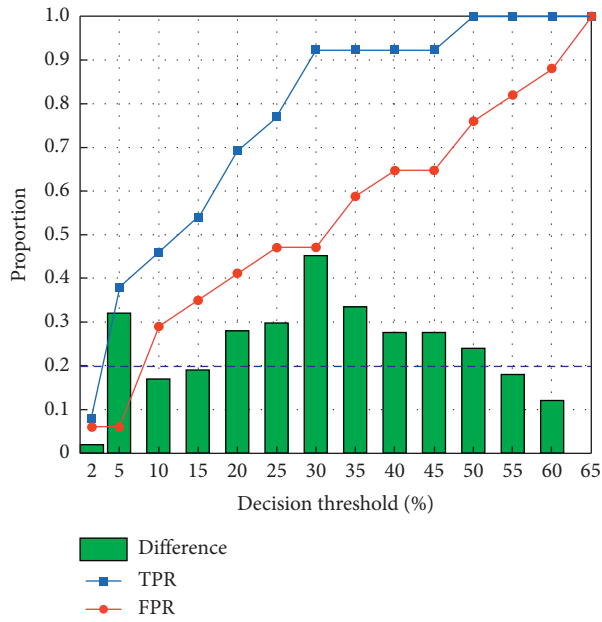
FIGURE 7: L - P_{cp} scatter diagram.



(a)

(b)

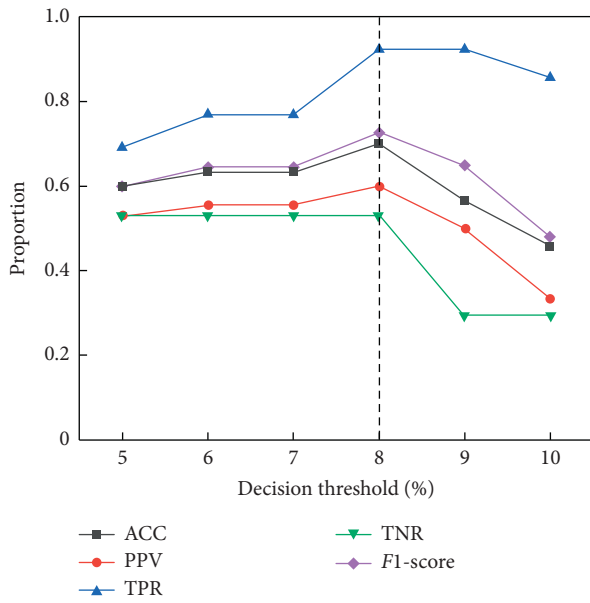
FIGURE 8: Continued.



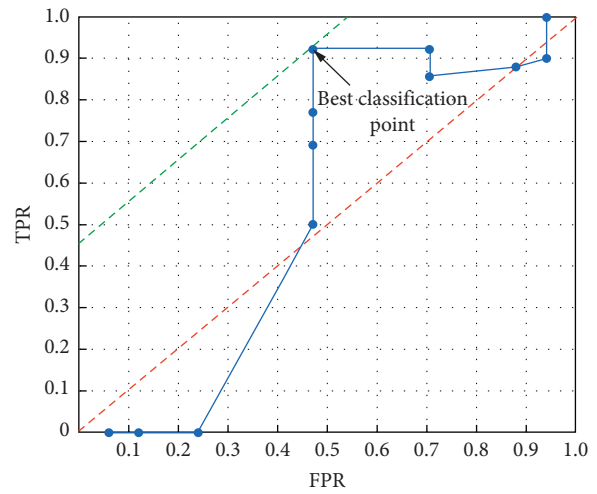
(c)

(d)

FIGURE 8: Variation curve of each evaluation index of P_{sp} . (a) Basic evaluation index curve. (b) ROC curve. (c) KS curve. (d) L - P_{sp} scatter diagram.

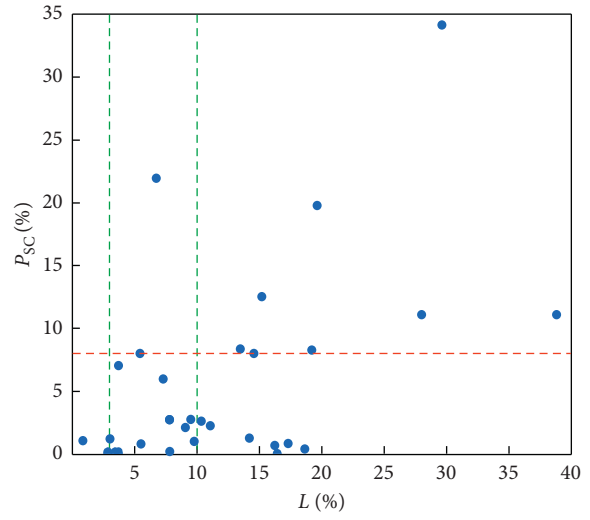
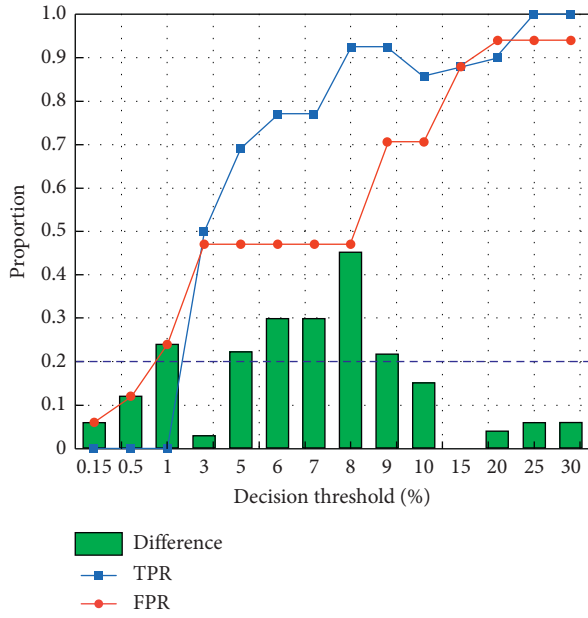


(a)



(b)

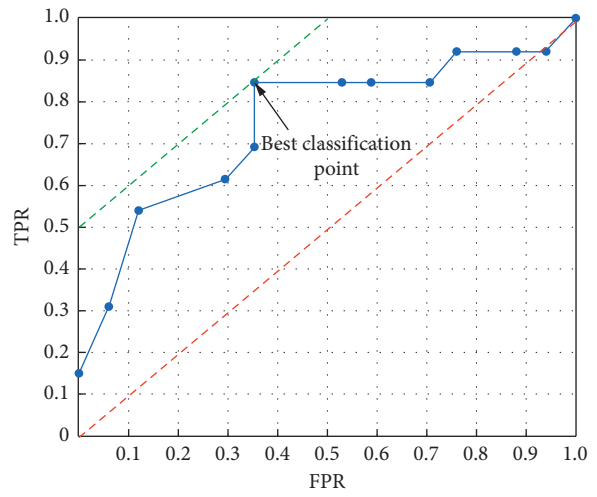
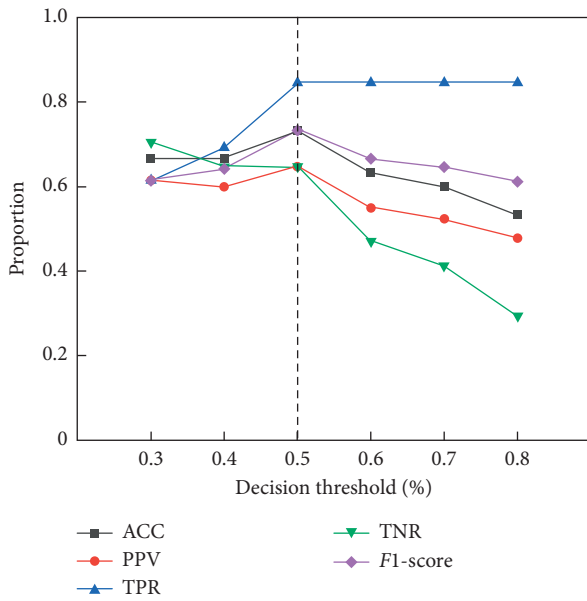
FIGURE 9: Continued.



(c)

(d)

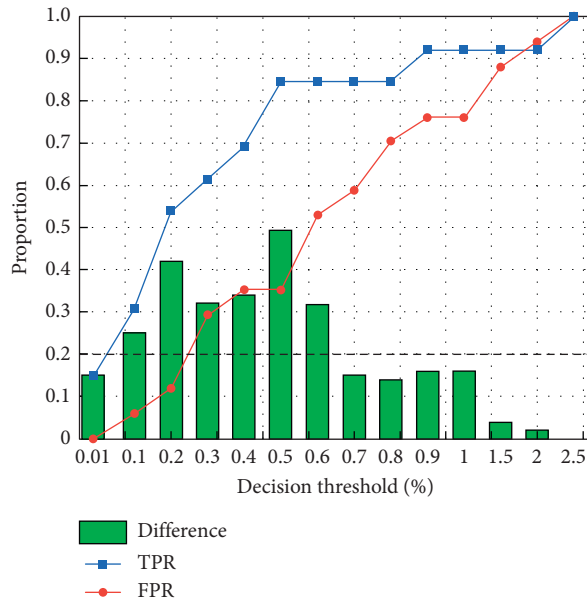
FIGURE 9: Variation curve of each evaluation index of P_{sc} . (a) Basic evaluation index curve. (b) ROC curve. (c) KS curve. (d) L - P_{sp} scatter diagram.



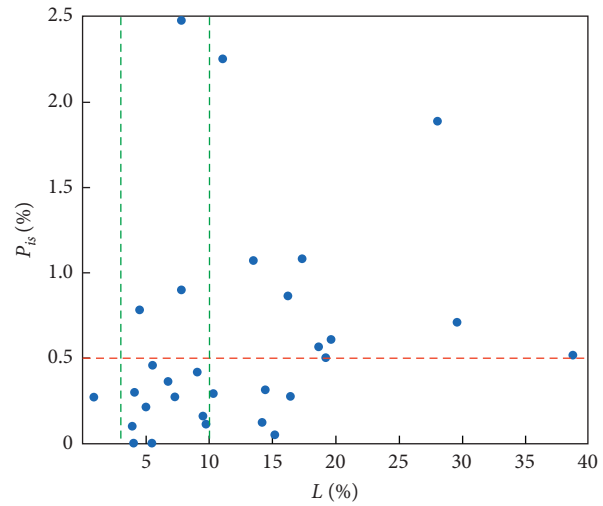
(a)

(b)

FIGURE 10: Continued.



(c)



(d)

FIGURE 10: Variation curve of each evaluation index of P_{1s} . (a) Basic evaluation index curve. (b) ROC curve. (c) KS curve. (d) L - P_{sp} scatter diagram.

basic evaluation index curve, ROC curve, and KS curve and scatter diagram of the three indexes are shown in Figures 8–10. The optimal threshold values of P_{sp} , P_{sc} , and P_{1s} are 30%, 8%, and 0.5%, respectively.

4.2.3. Determination of Dominant Distress Judgement Standard. Through the above analysis, the lower limit value of the judgement threshold of corner peeling rate, surface peeling rate, surface crack rate, and interplate slip rate was determined. When one of the four indexes is greater than the corresponding threshold value, the failure speed of pavement will be intensified. It is not suitable for the PM and requires medium repair or major repair. When the four indexes are at a good level because the corresponding indexes only represent a type of pavement distress, they cannot reflect the overall damage condition of pavement. It is impossible to judge whether the pavement needs PM from a single index, and it needs to be determined together with other indexes. Therefore, it is of no practical significance to set the upper limit value of a single index. After analysis, the judgement standard of the dominant distress of pavement PM were determined (corner peeling rate $\leq 35\%$, surface peeling rate $\leq 30\%$, surface crack rate $\leq 8\%$, and interplate slip rate $\leq 0.5\%$).

The judgement standard of each index determined in this paper can also be combined with the corresponding prediction model. After the solution, the corresponding PM time period is obtained, and then, the best time in PM of pavement is determined by the method of set theory. It can provide basis for pavement PM decision-making and promote the popularization and application of PM technology in pavement management of our military airport.

5. Conclusion

Preventive maintenance measures have obvious regional characteristics. Scientific and reasonable preventive maintenance research must be carried out in specific areas. In China, the seasonal frozen areas are widely distributed, with complex climate characteristics, a large number of airports, and complex distress characteristics. It is typical to select the seasonal frozen area as the preventive maintenance research area of this paper. On this basis, the research on the dominant distresses and its judgement standard of military airport cement concrete pavement based on preventive maintenance was carried out.

According to the survey data of the influential factors of pavement damage collected in this paper, the SEM was constructed and the path coefficient was estimated. The applicability and rationality of the model were verified by six statistical tests. It can be concluded that joint distresses, surface distresses, vertical distresses, repair distresses, and fracture distresses have a positive impact on pavement damage. After analyzing, the dominant distresses affecting the preventive maintenance of cement concrete pavement in military airports in the seasonal frozen area are corner peeling, surface peeling, surface crack, and interplate slip. The key content of the preventive maintenance research of the pavement is determined, which can provide a basis for the determination of the preventive maintenance judgement standard.

Based on the dominant distresses that affect the preventive maintenance of pavement, the confusion matrix model was constructed. The basic evaluation index, the ROC curve, and the KS curve were used to determine the pavement preventive maintenance judgement standard of corner peeling, surface peeling, surface crack, and interplate slip

from multiple evaluation angles. This judgement standard can be used to determine the best time for preventive maintenance of cement concrete pavement and provide pavement maintenance managers with the support of decision-making in the military airport. It can promote the scientific management of pavement maintenance and the establishment of an active pavement maintenance management system of the military airport.

However, this study has some limitations. These data are from military airports in Northeast China, such as Heilongjiang Province, Jilin Province, and Liaoning Province. The applicability of these data outside Northeast China is still uncertain. The specific parameters vary from different regions. The preventive maintenance judgement standard established in this paper also varies from place to place, which is only for reference. In practical application, corresponding adjustments should be adjusted according to the characteristics of different regions.

Data Availability

The data that support the findings of this study are available upon request from the corresponding author. The data are not publicly available due to their containing information that could compromise the privacy of research participants.

Conflicts of Interest

The authors declare that they have no conflicts of interest.

Authors' Contributions

Guanhu Wang was involved in funding acquisition. Qiqi Chen was involved in investigation. Qiqi Chen, Guanhu Wang, and Ke Li were involved in methodology. Qiqi Chen and Guanpeng Wang were involved in software. Qiqi Chen and Guanhu Wang were involved in writing—original draft. Qiqi Chen, Guanhu Wang, Xuelin Huang, Guanpeng Wang, and Ke Li were involved in writing—review and editing.

Acknowledgments

The authors would like to acknowledge all those who were involved in the field investigation on pavement distresses. This work was supported by the National Natural Science Foundation of China (Grant no. 51578540).

References

- [1] L. Jing, G. Q. Liu, T. Yang, J. Zhou, and Y. Zhao, "Research on relationships among different distress types of asphalt pavements with semi-rigid bases in China using association rule mining: a statistical point of view," *Advances in Civil Engineering*, vol. 2019, Article ID 5369532, 15 pages, 2019.
- [2] Z. Han, J. D. Porras-Alvarado, C. Stone, and Z. Zhang, "Incorporating uncertainties into determination of flexible pavement preventive maintenance interval," *Transportmetrica A: Transport Science*, vol. 15, no. 1, pp. 34–54, 2019.
- [3] C. S. Syan and G. Ramsoobag, "Maintenance applications of multi-criteria optimization: a review," *Reliability Engineering & System Safety*, vol. 190, p. 106520, 2019.
- [4] M. Putu, D. Colin, G. Thompson, and M. R. Wigan, "Measuring pavement maintenance effectiveness using Markov chains analysis," *Structure & Infrastructure Engineering: Maintenance, Management, Life-Cycle Design & Performance*, vol. 13, no. 7, pp. 844–854, 2017.
- [5] P. Arabali, M. Sakhaeifar, and T. Freeman, "Decision-making guideline for preservation of flexible pavements in general aviation airport management," *Journal of Transportation Engineering, Part B: Pavements*, vol. 143, no. 2, p. 04017006, 2017.
- [6] X. Q. Chen and H. H. Zhu, "Optimal Thresholds for pavement preventive maintenance treatments using LTPP data," *Journal of Transportation Engineering, Part A: Systems*, vol. 143, no. 6, p. 04017018, 2017.
- [7] A. Setyawan, J. Nainggolan, and A. Budiarto, "Predicting the remaining service life of road using pavement condition index," *Procedia Engineering*, vol. 125, pp. 417–423, 2015.
- [8] Q. Chen and G. Wang, "Research on relationships among different disease types of cement concrete pavement based on structural equation model," *Mathematical Problems in Engineering*, vol. 2020, Article ID 9580616, 13 pages, 2020.
- [9] Y. Y. Li, J. Y. Sun, and Y. Zhang, "Establishment and standard research of preventive maintenance index system for road pavement," *Journal of Highway and Transportation Research*, vol. 32, no. 3, pp. 52–57, 2016.
- [10] L. J. Wang, Z. H. Wang, J. H. Bai et al., "Integration of preventive maintenance time and countermeasures for asphalt pavement based on time period," *China Journal of Highway and Transport*, vol. 23, no. 5, pp. 27–34, 2010.
- [11] N. Zhang, "Critical range of key indicators for preventive maintenance of asphalt pavement," *Highway Traffic Technology*, vol. 4, p. 74, 2015.
- [12] X. Y. Fan, F. C. Gao, T. F. He, and H.-j. An, "Establishment of an evaluation model for asphalt pavement preventive maintenance based on improved EW-AHP," *Journal of Highway and Transportation Research and Development (English Edition)*, vol. 11, no. 3, 2017.
- [13] J. Yu, X. Zhang, and C. Xiong, "A methodology for evaluating micro-surfacing treatment on asphalt pavement based on grey system models and grey rational degree theory," *Construction and Building Materials*, vol. 150, pp. 214–226, 2017.
- [14] G. Loprencipe and P. Zoccali, "Comparison of methods for evaluating airport pavement roughness," *International Journal of Pavement Engineering*, vol. 20, no. 7, pp. 782–791, 2019.
- [15] N. Vu-Bac, T. Lahmer, X. Zhuang, T. Nguyen-Thoi, and T. Rabczuk, "A software framework for probabilistic sensitivity analysis for computationally expensive models," *Advances in Engineering Software*, vol. 100, pp. 19–31, 2016.
- [16] J. Chen and S. J. Li, "Mode choice model for public transport with categorized latent variables," *Mathematical Problems in Engineering*, vol. 2017, Article ID 7861945, 11 pages, 2017.
- [17] X. Gong, X. Guo, X. Dou, and L. Lu, "Bus travel time deviation analysis using automatic vehicle location data and structural equation modeling," *Mathematical Problems in Engineering*, vol. 2015, Article ID 410234, 9 pages, 2015.
- [18] S. M. Lu and C. Kang, "Analysing the organizational factors of project complexity using structural equation modelling," *International Journal of Project Management*, vol. 33, no. 1, pp. 165–176, 2015.
- [19] X. L. Bai, S. I. Niwas, W. S. Lin et al., "Learning ECOC code matrix for multiclass classification with application to glaucoma diagnosis," *Journal of Medical System*, vol. 40, no. 4, 2016.

- [20] P. Trajdos and M. Kurzynski, "A dynamic model of classifier competence based on the local fuzzy confusion matrix and the random reference classifier," *International Journal of Applied Mathematics and Computer Science*, vol. 26, no. 1, pp. 175–189, 2016.
- [21] D. Sisodia and D. S. Sisodia, "Prediction of diabetes using classification algorithms," *Procedia Computer Science*, vol. 132, pp. 1578–1585, 2018.
- [22] Ministry of Natural Resources of China, "Map of China by the ministry of natural resources of China [DB/OL]," 2020, <http://bzdt.ch.mnr.gov.cn/>.
- [23] R. Luca, P. Laura, S. Cristina et al., "Parenting stress, mental health, dyadic adjustment: a structural equation model," *Frontiers in Psychology*, vol. 8, p. 839, 2017.
- [24] G. Taraba, D. Gary, G. James et al., "The evolving relationship between casework skills, engagement, and positive case outcomes in child protection: a structural equation model," *Children and Youth Services Review*, vol. 79, pp. 456–462, 2017.
- [25] S. Tosunta, K. Engin, and O. Sevil, "The factors affecting acceptance and use of interactive whiteboard within the scope of FATIH project: a structural equation model based on the Unified Theory of acceptance and use of technology," *Computers & Education*, vol. 81, no. 1, pp. 169–178, 2015.
- [26] B. Kline, "Response to leslie hayduk's review of principles and practice of structural equation modeling, 4th edition," *Canadian Studys in Population*, vol. 45, no. 3-4, pp. 188–195, 2018.
- [27] J. F. Hair, G. T. M. Hult, C. M. Ringle, M. Sarstedt, and K. O. Thiele, "Mirror, mirror on the wall: a comparative evaluation of composite-based structural equation modeling methods," *Journal of the Academy of Marketing Science*, vol. 45, no. 5, pp. 616–632, 2017.
- [28] Q. Zou, S. Xie, Z. Lin et al., "Finding the best classification threshold in imbalanced classification," *Big Data Research*, vol. 5, pp. 2–8, 2016.
- [29] J. Kim, J. Lee, and Y. Lee, "Data-mining-based coronary heart disease risk prediction model using fuzzy logic and decision tree," *Healthcare Informatics Research*, vol. 21, no. 3, pp. 167–174, 2015.
- [30] P. Rajpurkar, A. Y. Hannun, M. Haghpanahi et al., "Cardiologist-level arrhythmia detection with convolutional neural networks," 2017, <https://arxiv.org/pdf/1707.01836.pdf>.
- [31] T. Baharia and M. Elayidomb, "An efficient CRM-data mining framework for the prediction of customer behaviour," *Procedia Computer Science*, vol. 46, pp. 725–731, 2015.
- [32] J. A. Cook, "ROC curves and nonrandom data," *Pattern Recognition Letters*, vol. 85, no. 1, pp. 35–41, 2017.
- [33] S. Takaya and R. Marc, "The precision-recall plot is more informative than the ROC plot when evaluating binary classifiers on imbalanced datasets," *PLoS One*, vol. 10, no. 3, Article ID e0118432, 2015.